

Preprocedural MRI and MRA in planning fibroid embolization

Cristina Maciel
Yen Zhi Tang
Anju Sahdev
António Miguel Madureira
Paulo Vilares-Morgado

ABSTRACT

This pictorial review aims to discuss and illustrate the up-to-date use of preprocedural magnetic resonance imaging (MRI) in selecting patients and planning uterine artery embolization (UAE). The merits of magnetic resonance angiography (MRA) in demonstrating the pelvic vasculature to guide UAE are highlighted. MRI features of fibroids and their main differential diagnoses are presented. Fibroid characteristics, such as location, size, and enhancement, which may impact patient selection and outcome, are presented based on recent literature. Pelvic arterial anatomy relevant to UAE, including vascular variants are illustrated, with conventional angiography and MRA imaging correlation. MRA preprocedural determination of the optimal projection angles for uterine artery catheterization is straightforward and constitutes an important strategy to minimize ionizing radiation exposure during UAE. A reporting template for MRI/MRA preassessment of UAE for fibroid treatment is provided.

Uterine artery embolization (UAE) has become a first-line treatment for symptomatic uterine fibroids alongside the conventional surgical treatment of hysterectomy and myomectomy. A 2014 Cochrane review including six randomized trials compared UAE versus hysterectomy or myomectomy for the treatment of symptomatic fibroids. UAE had similar short- and mid-term outcomes, such as symptom control, quality of life and patient satisfaction, while benefiting from uterine preservation, shorter hospital stay, and a shorter recovery before resuming activities of normal life (1). These benefits are in keeping with the minimally invasive nature of the embolization procedures.

Magnetic resonance imaging (MRI) is the best imaging modality to diagnose, map, and characterize fibroids. MRI can also diagnose benign and malignant concurrent pelvic pathology, which may also be attributing to symptoms. Some of these pathologies may preclude uterine artery embolization (UAE), or change the embolization protocol, such as the presence of adenomyosis.

There are absolute contraindications to fibroid embolization including a viable pregnancy, active uterine infection, and uterine or ovarian malignancy unless performed for palliation or as an adjunct to surgery (2).

For technically successful fibroid embolization, a microcatheter should be inserted into the uterine artery without complications, such as arterial spasm, dissection, or perforation. It is necessary to delineate the origin of the uterine artery, which is variable, and to understand its three-dimensional configuration. Although conventional angiography remains the gold standard for vascular evaluation, preprocedural three-dimensional (3D) magnetic resonance angiography (MRA) can give relevant preliminary information on uterine, ovarian, and pelvic vascular anatomy, shortening the operative time and increasing technical success rates. A reporting template for MRI/MRA preassessment of UAE for fibroid treatment is presented in the Table.

Evaluation of diagnostic pre-embolization MRI

Differentiation of fibroids from adenomyosis

Adenomyosis is characterized by the presence of heterotopic endometrial glands and stroma deep within the myometrium with adjacent myometrial hyperplasia (3). Adenomyosis is generally diffuse but focal adenomyosis and adenomyoma, a focal nodular form, also exist. Adenomyosis occasionally mimics fibroids and the two conditions can coexist (Fig. 1) (4). Concomitant adenomyosis in hysterectomy specimens of women with leiomyoma ranges from 15% to 57% (5).

From the Department of Radiology (C.M. ✉ tina_maciel@yahoo.com, A.M.M., P.V.M.), Centro Hospitalar São João, Porto, Portugal; the Department of Radiology (Y.Z.T., A.S.), St. Bartholomew's Hospital, London, UK.

Received 13 January 2016; revision requested 13 March 2016; last revision received 21 July 2016; accepted 30 July 2016.

Published online 6 February 2017.
DOI 10.5152/dir.2016.16623

Table. Reporting template for MRI/MRA preassessment of UAE for fibroid treatment

Items to report in preprocedural MRI/MRA examination

Uterus	Size (maximal length, width, and depth) Volume ($V = 0.52 \times \text{length} \times \text{width} \times \text{depth}$)
Fibroids	Number Size* Volume* ($V = 0.52 \times \text{length} \times \text{width} \times \text{depth}$) Location* Enhancement* Stalk diameter in pedunculated fibroids
Uterine arteries	Number, site of origin and size
Ovarian arteries	Number, site of origin and size
Suggested projection angle	For each uterine artery
Coexistence of adenomyosis	Classified as focal or diffuse
Additional pelvic pathologies	e.g., Adnexal masses, endometriosis, GI pathology, hydronephrosis

MRI/MRA, magnetic resonance imaging/magnetic resonance angiography; UAE, uterine artery embolization; GI, gastrointestinal.
*For the largest fibroids.



Figure 1. Coexistence of adenomyosis and a fibroid in a 54-year-old woman, presenting for pre-embolization evaluation. On initial ultrasonography (US), the patient was reported to have a large intramural fibroid in the anterior wall of the uterine body. Sagittal T2-weighted image shows thickening of the anterior junctional zone consistent with focal adenomyosis (Ad). A small intramural fibroid (F) is seen at the uterine fundus. The US features of adenomyosis and uterine fibroids overlap and can lead to incorrect diagnosis, as in this case.

Key imaging findings: Diffuse adenomyosis is most visible on T2-weighted sequences as ill-defined thickening of the junctional zone. There may be intralesional foci of T1 and/or T2 hyperintensities. A junctional zone 12 mm or greater in thickness is diagnostic of adenomyosis (3). Unlike fibroids, adenomyosis generally lacks distinct margins and exerts no mass effect. Instead of displacing or distorting the adjacent endometrium, adenomyosis abuts the endometrium (3).

Practical relevance to UAE: Patients with pure adenomyosis or adenomyosis coexist-

ing with fibroids are potential candidates for UAE. The presence of adenomyosis requires a more aggressive UAE technique, using smaller microspheres with an angiographic endpoint of complete stasis. In contrast, the endpoint for simple fibroids is near stasis, which is usually sufficient (6).

Differentiation of fibroids from uterine leiomyosarcoma

Uterine sarcomas are rare tumors, accounting for less than 3% of all female genital tract malignancies and for approximately 8% of uterine malignancies (7, 8). Leiomyosarcoma (LMS) is the most common histologic subtype of uterine sarcomas. Definitive differentiation of LMS from fibroids is not possible on imaging and ultimately diagnosis is made at histology. While some imaging features may help suggest LMS over fibroids, it is difficult to exclude LMS if this is suspected, particularly in the absence of metastases. However, it should be noted that in the majority of cases where LMS is suspected, histology usually reveals a benign fibroid (Fig. 2) (9). In rare cases, LMS will be inadvertently embolized. Inadvertent UAE treatment of LMS does not seem to spread malignancy, but this approach may impair prognosis by delaying diagnosis (7).

Key imaging findings: Imaging features suggesting LMS include a myometrial mass,

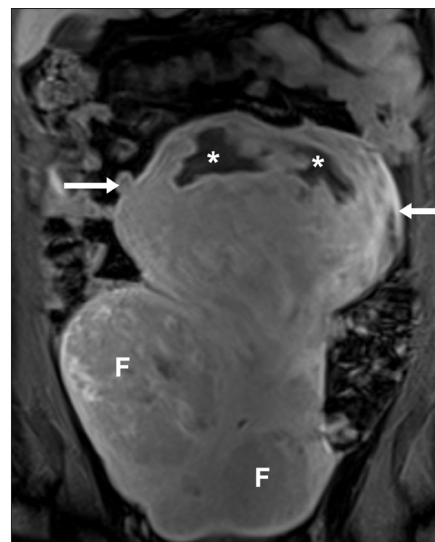


Figure 2. Suspicion of uterine leiomyosarcoma in a 31-year-old woman, presenting with epigastric pain and anorexia. The patient had undergone two previous uterine artery embolizations (UAEs). Coronal T2-weighted image obtained five years after the second UAE. The uterus is enlarged, extending to the upper abdomen. There is a bulky, heterogeneous mass (arrows) arising from the uterine fundus, with internal necrotic/cystic areas (asterisks). There are background uterine fibroids (F). Given the size and internal necrotic/cystic areas within the fundal lesion, the possibility of a leiomyosarcoma was raised. There was no evidence of metastatic disease. The patient underwent hysterectomy and histology revealed a fibroid.

Main points

- Uterine artery embolization (UAE) is a first-line treatment for symptomatic fibroids, with the benefits of uterine preservation and being minimally invasive.
- Fibroid location and enhancement can impact patient selection and outcome of UAE.
- Pelvic arterial variants relevant for UAE are not rare and can be delineated with preprocedural MRA.
- MRA provides the optimal projection angles for uterine artery catheterization, which enables the reduction of the UAE radiation dose.
- We highlight the relevant items to report in preprocedural MRI/MRA examination.

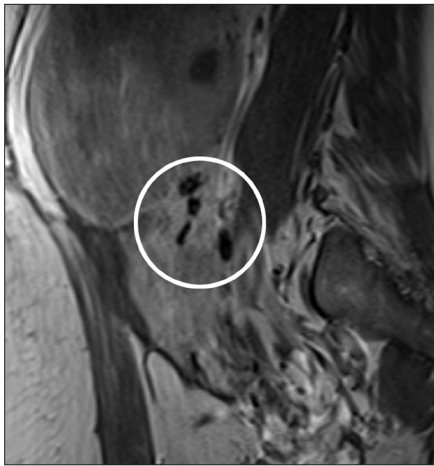


Figure 3. Pedunculated, subserosal fibroid in a 40-year-old woman, presenting for pre-embolization evaluation. The differential diagnosis was an adnexal mass on imaging. A bridging vessel sign is seen on the sagittal contrast-enhanced T1-weighted image. This is seen as multiple, curvilinear, tortuous flow voids representing vessels (*circled*) originating from the uterus, between the uterus and lesion. This sign enables confirmation that the mass is uterine in origin and a fibroid.

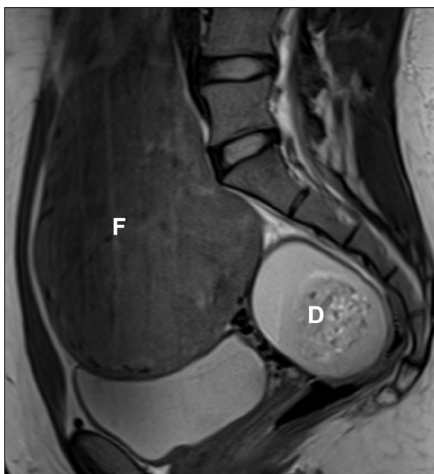


Figure 4. Coexistence of fibroids and dermoid cyst in a 33-year-old woman, presenting for pre-embolization evaluation. Sagittal T2-weighted image reveals a large fibroid (F). A complex, heterogeneous mass (D) is seen in the pouch of Douglas with mixed high T2 signal intensity. On further sequences it was demonstrated to arise from the right ovary. Additional T1-weighted fat-saturated contrast-enhanced image (not shown), demonstrated the presence of macroscopic fat, allowing the pre-embolization diagnosis of a mature dermoid cyst. Benign adnexal masses are not a contraindication for UAE.

usually large, with bizarre appearances, including intermediate-to-high T2 signal intensity (SI) with central hyperintensity indicative of necrosis (present in >50% of cases). There may be areas of high T1 SI representing hemorrhage. LMS may have early hetero-

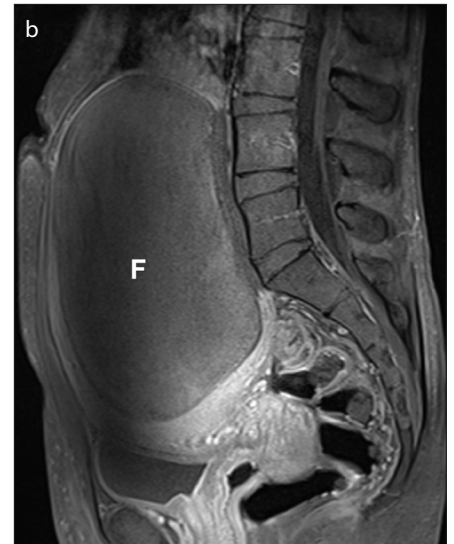


Figure 5. a, b. Successful UAE in a 33-year-old patient presenting with a huge fibroid measuring 16.5 cm in long axis (estimated volume 820 cc) on the pre-embolization MRI. Sagittal T1-weighted fat-saturated contrast-enhanced image (a) before UAE depicts a huge fibroid (F). Sagittal T1-weighted fat-saturated contrast-enhanced image (b) obtained three months after UAE, shows a still bulky fibroid (F), with complete lack of enhancement, consistent with successful devascularization by embolization. MRI examination one year after UAE shows additional reduction in size of the fibroid measuring 14.3 cm in long axis, with an estimated volume of 680 cc (not shown). At this point, the patient reported clinical improvement with resolution of pelvic pressure symptoms.

geneous enhancement resulting from the intratumoral necrosis and hemorrhage (8). The typical well-defined margin of fibroids is usually absent in LMS, while ill-defined, irregular margins are more likely to be seen in LMS (10). Rapid growth is often considered a suggestive feature of LMS, particularly in postmenopausal women. Postprocedural MRI follow-up is crucial to identify patients who do not respond predictably to UAE, as limited response or continued growth after embolization could suggest malignancy (7).

Practical relevance to UAE: imaging appearances suspicious of LMS should prompt consideration of short-interval follow-up imaging or surgical management.

Differentiation of fibroids from an adnexal mass

Differentiating between pedunculated subserosal fibroid and adnexal masses can be challenging, particularly when the ovaries are not confidently identified separately. Solid, low T2 SI, adnexal masses (e.g., fibromas, fibrothecomas, and Brenner tumors) can simulate pedunculated, subserosal fibroids. Pedunculated, subserosal fibroids with cystic degeneration can simulate complex, cystic, adnexal masses.

Key imaging findings: Establishing the uterine origin of a fibroid is key in differen-

tiating it from an adnexal mass. Features supporting uterine origin include splaying of myometrium around the lesion (the claw sign) and a bridge of feeding vessels arising from the myometrium, seen between the lesion and myometrium (the bridging vessel sign or bridging vascular sign) (Fig. 3) (11). Obtaining optimally angled sequences, such as with a uterine or ovarian axis, can also clarify the lesions' origin.

Practical relevance to UAE: It is important to differentiate adnexal masses from fibroids. Ovarian malignancy should be excluded prior to UAE. Benign ovarian lesions are not a contraindication to UAE (Fig. 4) (2).

Fibroid size

Several recent studies demonstrated clinically successful UAE in large fibroids and uterine volumes (defined as a dominant tumor with a long axis 10 cm or a uterine volume 700 cc or greater) comparable to results in smaller fibroids (Fig. 5). The UAE complication rate is unaffected by fibroid or uterine size (12, 13).

Key imaging findings: To obtain uterine or fibroid volume, the simplified formula $0.52 \times \text{length} \times \text{width} \times \text{depth}$ is used.

Practical relevance to UAE: Large fibroids and/or large uterine volumes due to

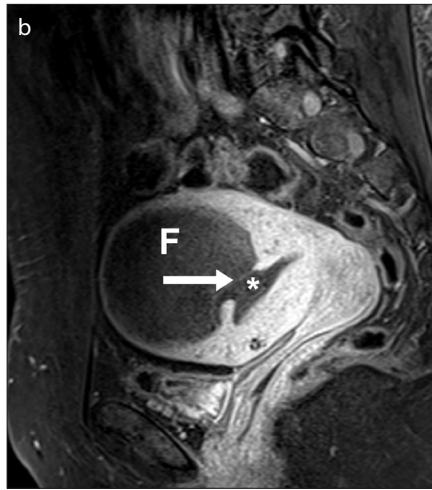


Figure 6. a, b. Sloughing of a treated fibroid three months after UAE in a 35-year-old woman. Sagittal T2-weighted image (a) before UAE shows a transmural fibroid (F) with an important submucosal component (arrows). Sagittal T1-weighted fat-saturated contrast-enhanced image (b) three months after UAE, demonstrates complete infarction of the fibroid. The posterior aspect of the fibroid is now contiguous with the endometrial canal and is beginning to pass (arrow) into the endometrial cavity (asterisk). This patient was clinically well, with no signs of infection on the images and therefore managed conservatively. However, patients with infarcted fibroids, contiguous with the endometrium, may have heavy bleeding per vagina, which may necessitate a hysterectomy.

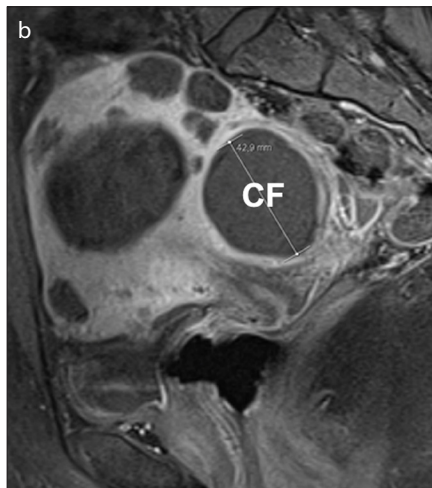
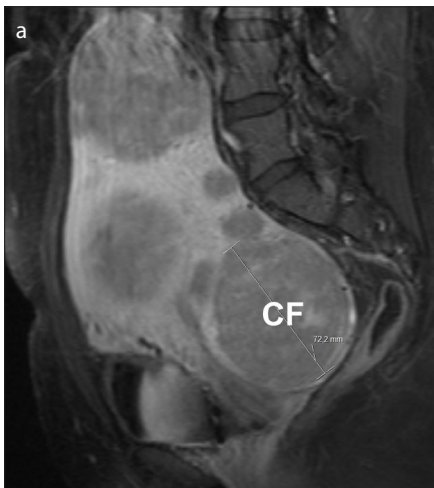


Figure 7. a, b. Cervical fibroid in a 32-year-old woman with multiple fibroids, undergoing successful embolization. Sagittal T1-weighted fat-saturated contrast-enhanced image (a) shows several, homogeneous, viable fibroids one of which is cervical in location (CF). After UAE, sagittal T1-weighted fat-saturated contrast-enhanced image (b) shows complete lack of enhancement of all fibroids, consistent with successful embolization. The cervical fibroid exhibits significant decrease in size, from 7.2 cm to 4.3 cm in long axis. The presence of cervical fibroids should be mentioned in the preprocedural MRI report, as they are more resistant to complete infarction than are other fibroid locations.

smaller fibroids should not exclude patients from UAE.

Fibroid location

Although all fibroid locations are eligible for embolization, certain anatomical fibroid subtypes deserve special consideration (14).

Submucosal location: Submucosal and intramural fibroids with a large submucosal component may be at increased risk of

post-UAE expulsion or sloughing (Fig. 6). This may cause uterine obstruction, pain, bleeding, infection, and prolonged vaginal discharge (15). If there is chronic bleeding from the devascularized fibroid and the endometrial cavity, a hysterectomy may be required. Conversely, sloughing may go unnoticed by patients.

Pedunculated subserosal fibroids: Traditionally, these have been considered a relative contraindication to UAE due to po-



Figure 8. Self-infarcted fibroids in a 33-year-old woman, presenting for pre-embolization evaluation. Sagittal T1-weighted fat-saturated contrast-enhanced image shows lack of enhancement of two fibroids (F1, F2). Since these fibroids are avascular, UAE is unlikely to decrease the fibroids' size or improve patient symptoms. F3 presents the most common enhancement pattern, being slightly hypovascular compared with the adjacent myometrium.

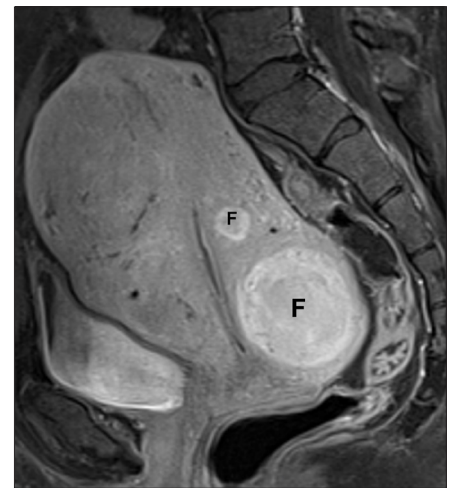


Figure 9. Hypervascular fibroids in a 33-year-old woman, presenting for pre-embolization evaluation. Sagittal T1-weighted fat-saturated contrast-enhanced image demonstrates marked enhancement of both intramural, hypervascular fibroids (F), which show greater enhancement than the myometrium. These findings are consistent with cellular fibroids.

tential risk of detachment, when the uterine pedicle is narrow (2). However, in two studies comprising of 28 patients with pedunculated, subserosal fibroids, no cases had fibroid detachment and clinical outcomes were comparable to patients with other fibroid locations (16,17).

Cervical fibroids: Cervical fibroids display similar features to fibroids in the uterus. They typically have low T1/T2 SI with a smooth capsule. Conversely, cervical

cancers have intermediate/high T2 signal, irregular borders and are readily visible against the background of cervical stroma with very low T2 signal.

Cervical fibroids appear to be more resistant to complete infarction after UAE. In a study of 10 patients with cervical fibroids the technical success of UAE was disappointing, with only two patients (20%) showing complete infarction (Fig. 7) (18). Incomplete infarction may be due to collateral blood supply to the cervix.

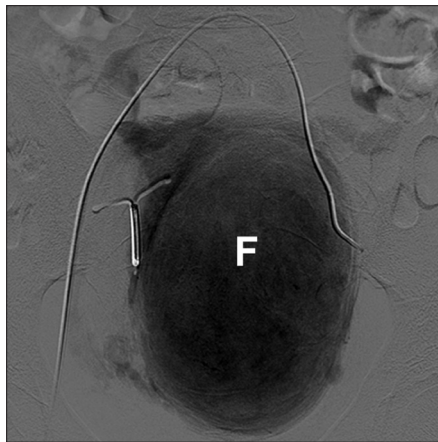


Figure 10. UAE in a 40-year-old patient having a copper-containing intrauterine device. Uterine angiogram obtained before embolization shows a large fibroid (F) projecting from the left side of the uterus. The intrauterine device remains *in situ*. The presence of an intrauterine device is not a contraindication to UAE.

Practical relevance to UAE: Patients should be informed of lower success rates and possible complications of UAE based on the location of the fibroids.

Enhancement of fibroids

Enhancement of fibroids depends on their vascularity.

Key imaging findings: Gadolinium-enhanced T1-weighted fat-saturated sequences are essential in demonstrating fibroid vascularity. Fibroid vascularity varies from virtually absent (Fig. 8) to marked enhancement (hypervascular) compared with adjacent myometrium. Cellular leiomyomas, made of compact smooth muscle cells with little or no collagen, have high T2-weighted SI with typically marked homogeneous enhancement postcontrast (Fig. 9) (19).

Practical relevance to UAE: Hypovascular fibroids may not show volume reduction with UAE, and therefore symptom relief is less likely (19). Fibroids with high T2-weighted SI and intense gadolinium enhancement tend to respond better to UAE, whereas fibroids with increased T1-weighted SI and less gadolinium uptake may not shrink significantly following UAE.

Intrauterine devices/systems: is it safe to perform MRI/UAE?

Copper-containing intrauterine devices (IUD) are safe for women scanned on a 1.5 T

system, with some models classified as MR conditional on a 3.0 T system (Fig. 10) (20). The Mirena (Bayer) intrauterine system (IUS) is a hormone-releasing device that contains levonorgestrel and is safe in all MRI magnetic field strengths. This T-shaped device is made of plastic, contains barium sulphate making it radiopaque, and does not contain copper.

The presence of an IUD/IUS has been traditionally considered a risk factor for postprocedural infection in patients undergoing UAE. However, in a small series of 20 patients undergoing UAE with an IUD/IUS *in situ*, there were no infectious complications. These patients received a prophylactic single-dose of antibiotics prior to UAE (21).

Practical relevance to UAE: The presence of IUD/IUS is not an absolute contraindication for UAE and its removal prior to UAE is not mandatory.

Evaluation of diagnostic pre-embolization MRA

UAE requires good knowledge of the variable origin of the uterine arteries. This is crucial to successful superselective catheterization, avoiding nontarget embolization, reducing radiation dose and shortening procedure time. MRA depicts uterine artery origin, demonstrates enlarged ovarian arteries, which may require embolization, and



Figure 11. a–c. Preprocedural MRI and MRA show an enlarged right uterine artery and a small caliber left uterine artery, in a 34-year-old woman presenting for fibroid embolization. 3D reconstructed MRA image (a) depicts a prominent right uterine artery (arrow). DSA (digital subtraction angiography) image (b) obtained with selective right internal iliac artery catheterization correlates with the MRA findings. Right parasagittal T2-weighted MRI image (c) shows flow voids (ellipse) appearing as hypointense structures at the interface between the fibroid (F) and the myometrium, in relation with dilated arterial branches with fast flow, feeding the vascular plexus of the fibroid. Right ovary has unremarkable appearance (asterisk).

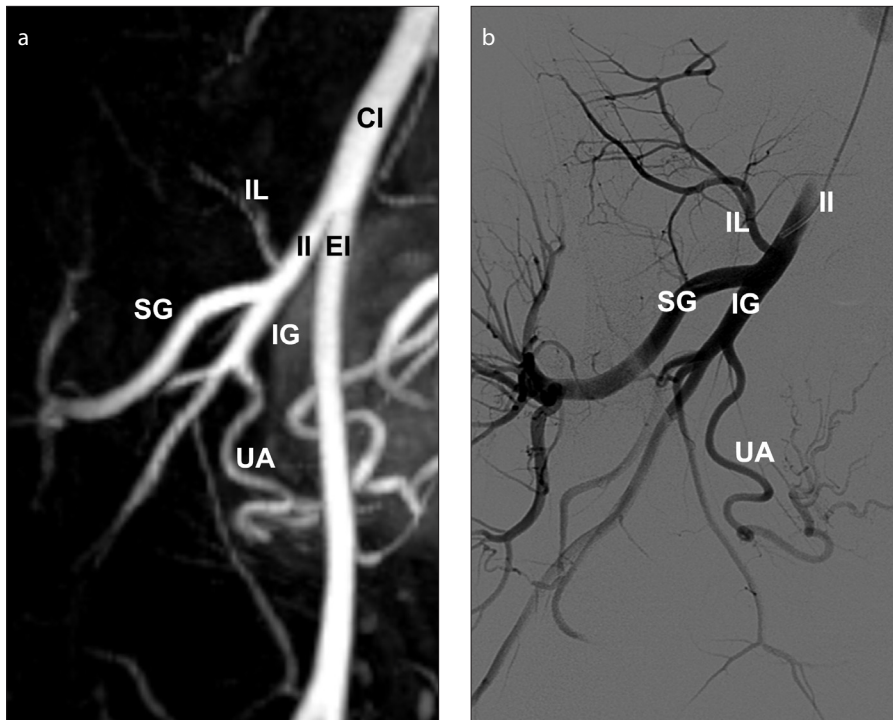


Figure 12. a, b. Preprocedural MRA with digital subtraction angiography (DSA) correlation shows a type I uterine artery origin, in a 31-year-old woman presenting for fibroid embolization. 3D reconstructed MRA image (a) depicts the uterine artery as the first branch of inferior gluteal artery. DSA image (b) obtained with selective internal iliac artery catheterization demonstrates good correlation with MRA findings. CI, common iliac; EI, external iliac; IG, inferior gluteal; IL, internal iliac; IL, iliolumbar; SG, superior gluteal; UA, uterine artery .

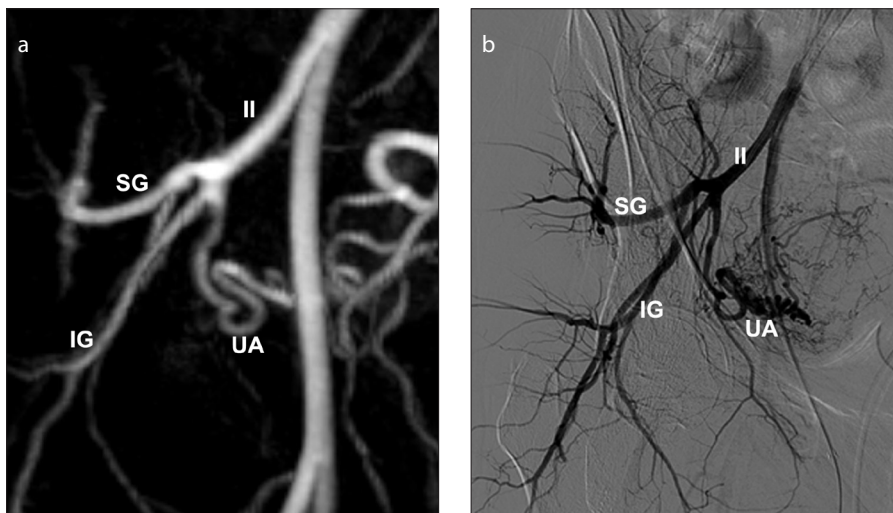


Figure 13. a, b. Preprocedural MRA with DSA correlation shows a type III uterine artery origin, in a 41-year-old woman. 3D reconstructed MRA image (a) clearly depicts the right uterine artery, inferior and superior gluteal arteries, originating at the same level from the internal iliac artery, as a trifurcation. DSA image (b) obtained with selective right internal iliac artery catheterization demonstrates good correlation with MRA findings. IG, inferior gluteal; II, internal iliac; SG, superior gluteal; UA, uterine artery.

reveals relevant anatomic variants, allowing for an adequate preprocedural planning.

Uterine artery

The uterine artery usually arises from the anterior division of the internal iliac artery and has a characteristic U shape. It has rich anastomoses with the ovarian and vagi-

nal arteries (22). The presence of uterine fibroids usually causes distortion and enlargement of the uterine arteries (Fig. 11).

Uterine artery origins

There is great variation in the branching patterns of the pelvic arteries. Conventionally, the internal iliac artery bifurcates into

anterior and posterior divisions. The anterior division gives rise to vesical, uterine, vaginal, and middle rectal arteries (visceral branches), obturator, inferior gluteal and internal pudendal arteries (parietal branches). The posterior division gives rise to iliolumbar, lateral sacral, and superior gluteal arteries (parietal branches) (23).

Gomez-Jorge et al. (24) formed a uterine artery origin classification system based on angiographic examinations. Type I is defined as the uterine artery arising as the first branch of the inferior gluteal artery (Fig. 12). In type II, the uterine artery branches off the inferior gluteal artery but not as the first branch. Type III is a true trifurcation, where the superior gluteal, inferior gluteal and uterine arteries originate at the same level (Fig. 13). In type IV, the uterine artery originates proximal to the bifurcation of the anterior and posterior divisions.

Uterine artery – anatomic variants

The congenital absence of one uterine artery has been reported with relative frequency (Fig. 14). According to two series, encompassing 2012 patients undergoing UAE for symptomatic fibroids, five cases of unilateral congenital absence were detected (incidence of 0.24%) (25, 26). When the uterine artery is absent, it is often replaced by the ipsilateral ovarian artery or may be replaced by small arterial pelvic branches (23). The congenital absence of both uterine arteries is very rare, with few case reports in the literature. In a case report unilateral ovarian artery embolization was performed in a 49-year-old patient with congenital absence of both uterine arteries, with substantial clinical improvement and complete infarction of the fibroids (27).

Ovarian artery

Both ovarian arteries arise from the abdominal aorta a few centimeters inferior to the renal arteries in 80%–90% of cases and have a characteristic corkscrew appearance (23).

Identification of the normal ovarian arteries is usually not possible with MRA and standard flush aortography because of their small diameter (usually less than 1 mm) (Fig. 15 a, 15b) (23).

Ovarian artery – anatomic variants

Rarely, the ovarian artery arises from the renal, accessory renal, lumbar, adrenal, inferior mesenteric, common iliac or external iliac arteries (Fig. 16) (28–30).

Enlarged ovarian artery

Collateral ovarian artery supply of fibroids is a cause of incomplete infarction of fibroids and subsequent clinical failure of the procedure. The identification of en-

larged ovarian arteries at MRA (Fig. 15b, 15c) can be helpful for prediction of adjunct ovarian artery embolization (OAE), particularly if combined with small or nonvisible uterine artery on MRA (31).

Practical relevance to UAE: Identifying enlarged ovarian arteries prior to UAE is important as these may require embolization. Awareness regarding ovarian artery origin variants is essential for successful catheterization and embolization. Patients should be counseled and consented for OAE as it may result in ovarian dysfunction, although this topic is controversial (32).

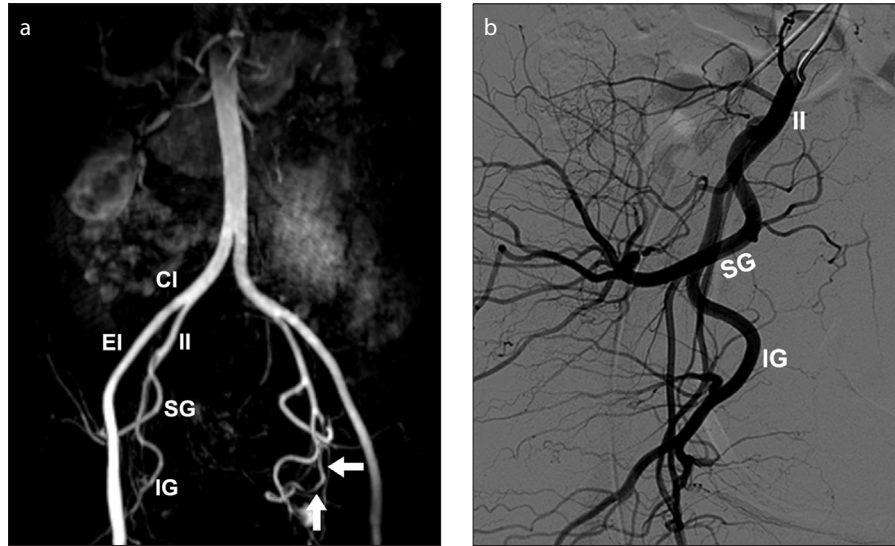


Figure 14. a, b. Absence of the right uterine artery in a 37-year-old woman, presenting for fibroid embolization. 3D reconstructed MRA image (a) shows absence of right uterine artery. The left uterine artery has normal morphology (arrows). No ovarian artery collateral supply to the uterus is seen. Absence of the right uterine artery was confirmed by selective internal iliac artery catheterization DSA (b). Additional arteries visualized include the common iliac (CI), external iliac (EI), internal iliac (II), superior gluteal (SG) and inferior gluteal (IG).

Extrauterine, extraovarian collateral supply to fibroids

Rarely, fibroids may recruit additional blood supply from the inferior mesenteric, superior mesenteric, and round ligament arteries. In a retrospective study of 509 patients who underwent UAE for uterine fibroids or adenomyosis, the inferior mesenteric artery was the most common extraovarian source of collaterals to the uterus and was seen in seven patients (1.3%) (33).

Practical relevance to UAE: The presence of aberrant branches not embolized, continuing to perfuse the fibroids or uterus, is a likely cause for treatment failure and MRA could be helpful in detecting this aberrant fibroid arterial supply.

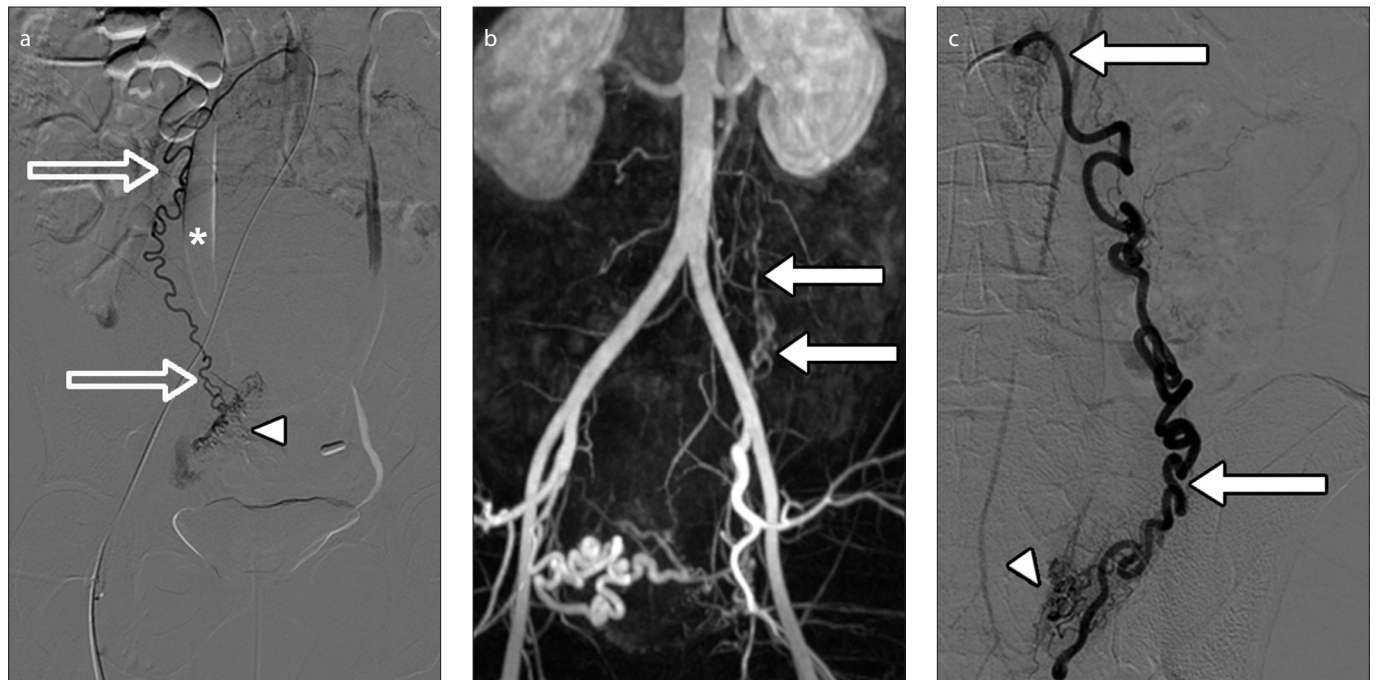


Figure 15. a–c. Visibility of ovarian arteries at MRA with DSA correlation, in a 34-year-old woman presenting for fibroid embolization. DSA image (a) obtained with selective right ovarian artery catheterization clearly depicts this artery. 3D reconstructed MRA image (b) reveals an enlarged left ovarian artery (arrows) extending from the aorta to the pelvis; the right ovarian artery is not seen due to its normal caliber. DSA image (c) obtained with selective left ovarian artery catheterization confirms the MRA finding of an enlarged left ovarian artery (arrows). At selective ovarian arteriography (a, c), ovarian parenchymal blush is present bilaterally (arrowheads) but no fibroid vascular blush was demonstrated. Note bilateral hydronephrosis (a), more marked in the right side (asterisk), likely related to the obstruction from the bulky fibroid (not shown).

Optimal projection angle for angiographic selection of the uterine arteries

The usual direction of tube obliquity (right anterior oblique view for the left uterine artery and left anterior oblique view for the right uterine artery) may fail to demon-

strate the uterine artery origin, regardless of the angle used. No standard angle can be recommended for all patients (34).

Practical relevance to UAE: MRA can assist the interventional radiologist with the

optimal projection angle for angiographic selection of each uterine artery, in each patient (Fig. 17). This is instrumental for efficient catheterization.

MRA and ionizing radiation exposure optimization during UAE

As the uterus and ovaries are directly exposed to the radiation beam during UAE, radiation exposure and risk have to be considered, particularly in females of reproductive age. Although the ovarian doses are below the threshold for temporary or permanent sterility and the stochastic risk for radiation-induced cancer and genetic injury to the patient's future children is not considered substantial (35), strategies for dose optimization should be utilized.

To minimize radiation exposure, a preprocedural MRA can identify enlarged ovarian arteries avoiding the final aortogram, and predict the optimal projection angle for angiographic selection of the uterine arteries. Naguib et al. (34), demonstrated a 62% reduction in overall radiation dose, a 43% reduction in fluoroscopy time and a 44% reduction in contrast medium volume used when using preprocedural MRA for determining optimal projection angles for the angiographic selection of uterine arteries.

Conclusion

MRI and MRA have multifaceted roles in correctly selecting patients and planning UAE for fibroids. MRI allows accurate diagnosis and mapping of fibroids, excludes coexisting pelvic pathology, and provides

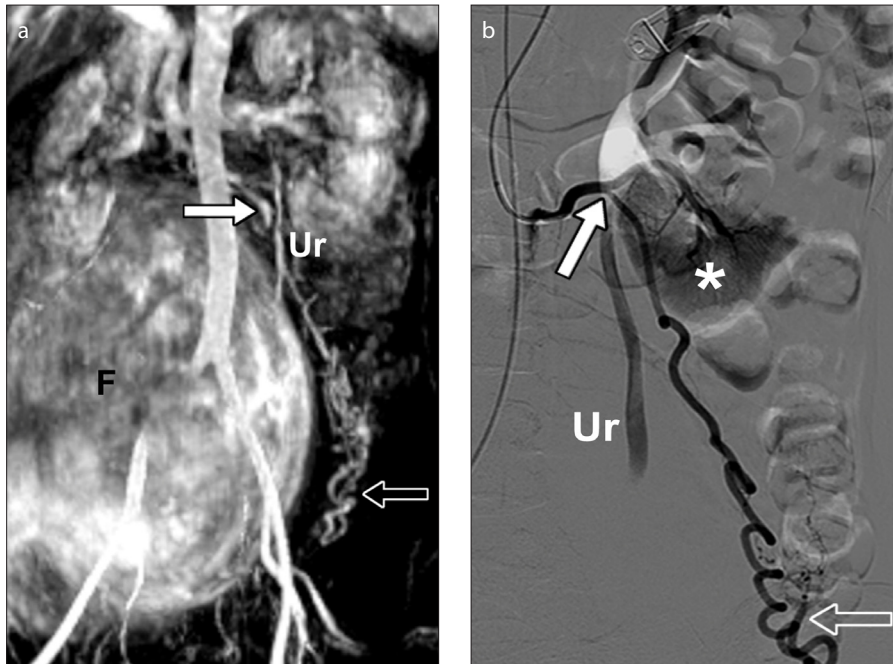


Figure 16. a, b. Left ovarian artery arising from an accessory left renal artery in a 34-year-old woman, presenting for fibroid embolization. Maximum intensity projection image (a) from MRA shows an enlarged left ovarian artery (arrow) arising from an accessory lower pole renal artery. Notice the characteristic corkscrew appearance of the ovarian artery (open arrow). A huge fibroid (F) is seen in the background. The left ovarian artery does not contribute to the vascular supply of the fibroid. DSA image (b) obtained with selective accessory left renal artery catheterization confirms aberrant origin of the left ovarian artery. The arrow points to an enlarged left ovarian artery arising from an accessory left renal artery, showing the characteristic corkscrew appearance (open arrow). No ovarian artery supply to the fibroid or the uterus is demonstrated. The lower renal pole (asterisk) is depicted. Ur, ureter.

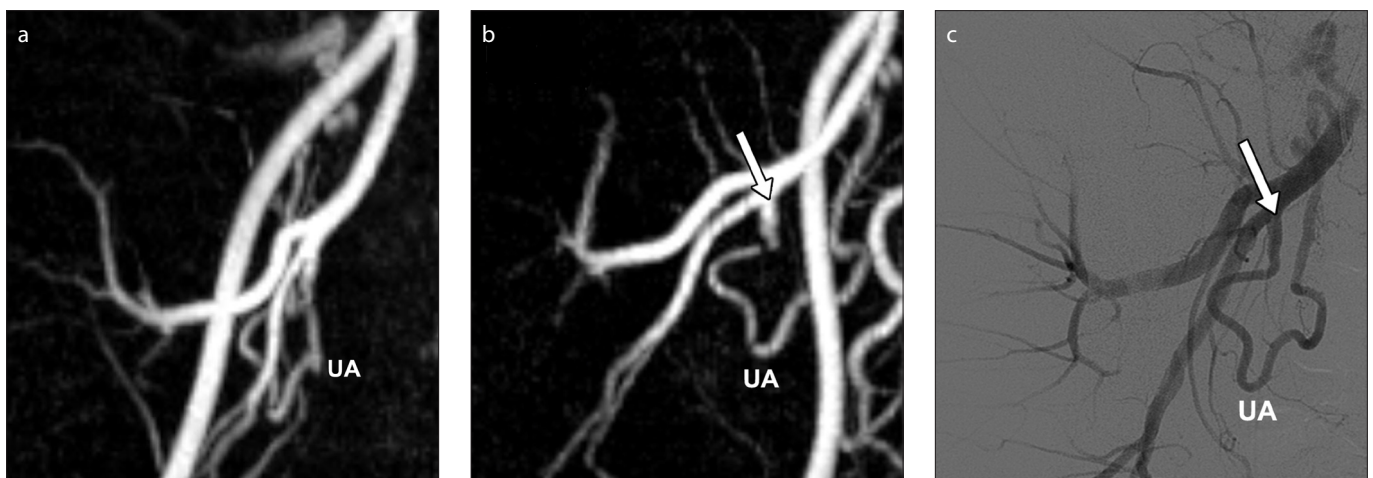


Figure 17. a–c. Assessment of optimal projection angle for angiographic catheterization of the uterine arteries with MRA, in a 40-year-old woman presenting for pre-embolization evaluation. 3D reconstructed MRA image (a) in a frontal view could not depict the origin of the right uterine artery. The model was then rotated to a 38° right obliquity (b) (contrary to the usual left oblique view used for the right uterine artery) for demonstration of the origin (arrow) of the right uterine artery. DSA image (c) shows the corresponding angiographic projection and clearly depicts the origin (arrow) of the right uterine artery. The assessment of the projection angle for angiographic catheterization of uterine artery is straightforward and should be tailored individually, as illustrated in this example.

technical information for planning UAE. MRA is used for comprehensive, pretreatment assessment of pelvic arterial anatomy, which ensures the technical success of the embolization procedure. Moreover, MRA reduces the radiation exposure during UAE, an important consideration, particularly in females of reproductive age.

Acknowledgements

We thank Sergio Ferreira for his administrative support.

Conflict of interest disclosure

The authors declared no conflicts of interest.

References

- Gupta JK, Sinha A, Lumsden MA, Hickey M. Uterine artery embolization for symptomatic uterine fibroids. *Cochrane Database Syst Rev* 2014; 12:Cd005073. [CrossRef]
- van Overhagen H, Reekers JA. Uterine artery embolization for symptomatic leiomyomata. *Cardiovasc Intervent Radiol* 2015; 38:536–542. [CrossRef]
- Kim MD, Kim S, Kim NK, et al. Long-Term Results of Uterine Artery Embolization for Symptomatic Adenomyosis. *AJR Am J Roentgenol* 2007; 188:176–181. [CrossRef]
- Sudderuddin S, Helbren E, Telesca M, Williamson R, Rockall A. MRI appearances of benign uterine disease. *Clin Radiol* 2014; 69:1095–1104. [CrossRef]
- Taran F, Weaver A, Coddington C, Stewart E. Characteristics indicating adenomyosis coexisting with leiomyomas: a case control study. *Hum Reprod* 2010; 25:1177–1182. [CrossRef]
- Nijnenhuis RJ, Smeets AJ, Morpurgo M, et al. Uterine artery embolisation for symptomatic adenomyosis with polyzene F-coated hydrogel microspheres: three-year clinical follow-up using UFS-QoL questionnaire. *Cardiovasc Intervent Radiol* 2015; 38:65–71. [CrossRef]
- Kainsbak J, Hansen ES, Dueholm M. Literature review of outcomes and prevalence and case report of leiomyosarcomas and non-typical uterine smooth muscle leiomyoma tumors treated with uterine artery embolization. *Eur J Obstet Gynecol Reprod Biol* 2015; 191:130–137. [CrossRef]
- Santos P, Cunha TM. Uterine sarcomas: clinical presentation and MRI features. *Diagn Interv Radiol* 2015; 21:4–9. [CrossRef]
- Brown DL. Uterine Leiomyomas. In: Fielding JR, Brown DL, Thurmond AS, eds. *Gynecologic imaging*. Philadelphia: Elsevier, 2011; 247. [CrossRef]
- Schwartz LB, Zawin M, Carcangiu ML, Lange R, McCarthy S. Does pelvic magnetic resonance imaging differentiate among the histologic subtypes of uterine leiomyomata? *Fertil Steril* 1998; 70:580–587. [CrossRef]
- Madan R. The bridging vascular sign. *Radiology* 2006; 238: 371–372. [CrossRef]
- Parthipun AA, Taylor J, Manyonda I, Belli AM. Does size really matter? Analysis of the effect of large fibroids and uterine volumes on complication rates of uterine artery embolisation. *Cardiovasc Intervent Radiol* 2010; 33:955–959. [CrossRef]
- Smeets AJ, Nijnenhuis RJ, van Rooij WJ, et al. Uterine artery embolization in patients with a large fibroid burden: long-term clinical and MR follow-up. *Cardiovasc Intervent Radiol* 2010; 33:943–948. [CrossRef]
- Bulman JC, Ascher SM, Spies JB. Current concepts in uterine fibroid embolization. *Radiographics* 2012; 32:1735–1750. [CrossRef]
- Kirby JM, Burrows D, Haider E, Maizlin Z, Midia M. Utility of MRI before and after uterine fibroid embolization: why to do it and what to look for. *Cardiovasc Intervent Radiol* 2011; 34:705–716. [CrossRef]
- Margau R, Simons ME, Rajan DK, et al. Outcomes after uterine artery embolization for pedunculated subserosal leiomyomas. *J Vasc Interv Radiol* 2008; 19:657–661. [CrossRef]
- Katsumori T, Akazawa K, Mihara T. Uterine artery embolization for pedunculated subserosal fibroids. *AJR Am J Roentgenol* 2005; 184:399–402. [CrossRef]
- Kim MD, Lee M, Jung DC, et al. Limited efficacy of uterine artery embolization for cervical leiomyomas. *J Vasc Interv Radiol* 2012; 23:236–240. [CrossRef]
- Deshmukh SP, Gonsalves CF, Guglielmo FF, Mitchell DG. Role of MR imaging of uterine leiomyomas before and after embolization. *Radiographics* 2012; 32:251–281. [CrossRef]
- Shellock FG. MRIsafety.com. <http://www.mrisafety.com/list.asp/>. Accessed November 29, 2015.
- Smeets AJ, Nijnenhuis RJ, Boekkooi PF, Vervest HAM, van Rooij WJ, Lohle PNM. Is an intrauterine device a contraindication for uterine artery embolization? A study of 20 patients. *J Vasc Interv Radiol* 2010; 2:272–274. [CrossRef]
- Maclaran KA, Edmonds DK, Tait P. Absence of uterine arteries discovered at fibroid embolisation. *Br J Radiol* 2009; 82:228–230. [CrossRef]
- Pelage J-P, Cazejust J, Pluot E, et al. Uterine fibroid vascularization and clinical relevance to uterine fibroid embolization. *Radiographics* 2005; 25:99–117. [CrossRef]
- Gomez-Jorge J, Keyoung A, Levy EB, Spies JB. Uterine artery anatomy relevant to uterine leiomyomata embolization. *Cardiovasc Intervent Radiol* 2003; 26:522–527. [CrossRef]
- Bratby MJ, Hussain FF, Walker WJ. Outcomes after unilateral uterine artery embolization: a retrospective review. *Cardiovasc Intervent Radiol* 2008; 31:254–259. [CrossRef]
- McLucas B, Reed RA, Goodwin S, et al. Outcomes following unilateral uterine artery embolisation. *Br J Radiol* 2002; 75:122–126. [CrossRef]
- Barth MM, Spies JB. Ovarian artery embolization supplementing uterine embolization for leiomyomata. *J Vasc Interv Radiol* 2003; 14:1177–1182. [CrossRef]
- Smoger DL, Kancherla V, Shlansky-Goldberg RD. Uterine fundal blood supply from an aberrant left ovarian artery originating from the inferior mesenteric artery: implications for uterine artery embolization. *J Vasc Interv Radiol* 2010; 21:941–944. [CrossRef]
- Kwon JH, Kim MD, Lee K-H, et al. Aberrant ovarian collateral originating from external iliac artery during uterine artery embolization. *Cardiovasc Intervent Radiol* 2013; 36:269–271. [CrossRef]
- Bensalah J, Dumoussat E, Niro J, et al. Aberrant ovarian and uterine feeding from the renal artery at the end of gestation: two cases. *J Vasc Interv Radiol* 2010; 21:1911–1912. [CrossRef]
- Lee MS, Kim MD, Lee M, et al. Contrast-enhanced MR angiography of uterine arteries for the prediction of ovarian artery embolization in 349 patients. *J Vasc Interv Radiol* 2012; 23:1174–1179. [CrossRef]
- Hu NN, Kaw D, McCullough MF, Nsouli-Maktabi H, Spies JB. Menopause and menopausal symptoms after ovarian artery embolization: a comparison with uterine artery embolization controls. *J Vasc Interv Radiol* 2011; 22:710–715. [CrossRef]
- Chang S, Lee MS, Kim MD, et al. Inferior mesenteric artery collaterals to the uterus during uterine artery embolization: prevalence, risk factors, and clinical outcomes. *J Vasc Interv Radiol* 2013; 24:1353–1360. [CrossRef]
- Naguib NN, Nour-Eldin N-EA, Lehnert T, et al. Uterine artery embolization: optimization with preprocedural prediction of the best tube angle obliquity by using 3D-reconstructed contrast-enhanced MR angiography. *Radiology* 2009; 251:788–795. [CrossRef]
- Glomset O, Hellesnes J, Heimland N, Hafsaht G, Smith HJ. Assessment of organ radiation dose associated with uterine artery embolization. *Acta Radiol* 2006; 47:179–185. [CrossRef]